Magnetic mesoporous carbon for efficient removal of organic pollutants

Tongbao Wang · Lin Liang · Runwei Wang · Yanqiu Jiang · Kaifeng Lin · Jianmin Sun

Abstract Carbon materials such as activated carbons have been used in the field of water and wastewater treatments. However, the lack of mesopore and, particularly, the difficulty in recovering the spent carbon limited their applications. In this work, magnetic mesoporous carbon microspheres were synthesized by impregnating iron oxide precursors in the mesoporous carbon followed by the in situ conversion of the precursors into magnetite nanoparticles. The as-synthesized carbon microspheres with a high surface area of 742 m^2/g and large mesopores of ∼4.4 nm exhibited an excellent adsorption capacity for aqueous organic pollutants. The superparamagnetic microspheres with a saturation magnetization of 7.15 emu/g can be easily separated from the treated solution by external magnetic field.

Keywords Magnetic · Mesoporous carbon · One-pot synthesis · Adsorption · Organic pollutant

J. Sun (✉)
State Key Laboratory of Urban Water Resource and Environment, Harbin Institute of Technology, Harbin 150090, China
e-mail: sunjm@hit.edu.cn

T. Wang · Y. Jiang · K. Lin · J. Sun
Natural Science Research Center, The Academy of Fundamental and Interdisciplinary Science, Harbin Institute of Technology, Harbin 150080, China

L. Liang
School of Life Science and Technology, Harbin Institute of Technology, Harbin 150080, China

R. Wang
State Key Laboratory of Inorganic Synthesis and Preparative Chemistry, College of Chemistry, Jilin University, Changchun 130012, China

1 Introduction

The Earth's water resources are being increasingly contaminated along with the rapid developments of industry and agriculture, which pose a major environmental health risk to humankind. Particularly, the effluents from textile plants containing portions of dyes, which are deeply colored, non-biodegradable and high toxic, have caused increasing environmental concerns (Lewis et al. 1999). Removal of pollutants by adsorption is clearly one of the most effective, economical and easily regenerated ways for environmental clean-up compared to other methods such as chemical precipitation, liquid-liquid extraction, membrane filtration, ion exchange (Li et al. 2005; Zhang et al. 2009; Mansouri et al. 2010). Mesoporous carbon materials with uniform porosity, high surface area, large pore volume, good thermal stability and chemical inertness, have gained increasing attentions in catalysis, adsorption, host-guest chemistry, environmental technology, and biomedical fields (Joo et al. 2001; Liang et al. 2008). However, it is difficult to separate mesoporous carbon materials from liquid phase because of their small particle sizes. A way to solve this is to induce magnetic nanomaterials into mesoporous carbon materials. The magnetic mesoporous carbon materials attract great interests in many fields because of their unique properties (Zhao et al. 2003; Son et al. 2005; Sun et al. 2006; Gao et al. 2007; Deng et al. 2011; Liu et al. 2011; Zhang et al. 2011; Wu et al. 2012). There are generally two routes to synthesize magnetic mesoporous carbon. One route is the "one-pot" block-copolymer self-assembly strategy associated with direct carbonization from carbon source, metal salt and block copolymers (Zhai et al. 2009; Wang and Dai 2009; Yao et al. 2009). Zhai et al. fabricated mesoporous γ-Fe_2O_3/carbon composites by the self-assembly method (Zhai et al. 2009). The other route is the nanocasting strategy by infiltration

of carbon precursors and metal source into the mesopores of the silica template, followed by thermal polymerization, and subsequent removal of the silica framework. Co nanoparticles were successfully immobilized onto the ordered mesoporous CMK-3. The mesocellular carbon foam was then used as magnetically separable adsorbents and hydrogenation catalyst support (Lu et al. 2004). Likewise, Fe_2O_3 nanoparticles were encapsulated into CMK-3 and carbon nanocages (Souza et al. 2008). Tian et al. developed a facile route for incorporation of superparamagnetic Fe_3O_4 nanoparticles onto the external surface of mesoporous carbon CMK-3 (Tian et al. 2007). Guo and coworkers synthesized magnetically separable mesoporous carbon composites by integrating carbon-coated magnetic particles onto the mesoporous carbon particle surface via cocasting method (Guo et al. 2009). Despite of considerable progress in the synthesis of mesoporous carbon, there is still no reliable process of introduction of magnetite into mesoporous carbon while retaining their porous structure (Liu et al. 2006). The reduced surface area and pore volume resulted from the pore clogging, the amorphous pore wall of the mesoporous materials, the complicated multistep synthetic process, and the low loadings of magnetic composite restrict their applications. A facile synthesis of magnetic mesoporous carbon with high surface area, large pore volume and strong magnetic responsiveness is desired. Herein, we developed a "one-pot" synthesis route to magnetic mesoporous carbon by impregnating iron oxide precursors into the mesoporous carbon followed by in situ conversion of the precursors into magnetic nanoparticles. The as-prepared magnetic mesoporous carbon material showed a remarkably enhanced adsorption rate, higher adsorption capacity and higher removal efficiency for organic pollutants from aqueous solution compared with Fe_3O_4 coated with amorphous carbon. Furthermore, magnetic mesoporous carbon material can be easily separated from the liquid phase after adsorption, which is very important in water treatment application.

2 Experimental

2.1 Chemicals

$FeCl_3 \cdot 6H_2O$, sodium acetate, ethylene glycol, tetraethylorthosilicate (TEOS), glucose, sucrose, polyethylene glycol (PEG Mw = 1500), active carbon (AC, BET 430.8 m^2/g) were purchased from Sinopharm Chemical Reagent Co. Ltd, China. PEO-PPO-PEO (P123) was supplied from Sigma-Aldrich.

2.2 Synthesis procedure

The preparation of the mesoporous carbon material was conducted by following the procedures in literature (Zhao et al.

1998; Jun et al. 2000). 1.08 g $FeCl_3 \cdot 6H_2O$ and 2.88 g sodium acetate were dissolved in 40 mL of ethylene glycol under magnetic stirring for 4 h at room temperature to afford a homogeneous yellow iron oxide precursor solution. Then 0.1 g mesoporous carbon was stirred with 5 mL of pre-synthesized iron oxide precursor solution, the slurry mixture was transferred into a Teflon-lined stainless autoclave and heated at 200 °C for 12 h. The obtained black product (denoted Fe/MC) was collected with magnet, washed with deionized water and ethanol, each for three times.

For comparison, Fe_3O_4 coated with amorphous carbon denoted Fe/C was synthesized as follows: Fe_3O_4 nanoparticles were synthesized as described in the literature (Zhang et al. 2008). 0.1 g Fe_3O_4 sample was treated with 70 mL 0.1 M HCl solution by ultrasonication for 15 min, then separated and washed with deionized water. Afterwards it was homogenously dispersed in the mixture containing 8 g glucose, 0.5 g PEG and 40 mL deionized water. The resultant solution was ultrasonicated and mechanically stirred for 40 min. The obtained solution was then transferred into a Teflon-lined stainless autoclave at 180 °C for 14 h. The black products were collected with magnet, washed with deionized water and ethanol, then dried in oven at 60 °C for 12 h. Finally, the products were carbonized at 900 °C for 6 h under N_2 flow.

2.3 Adsorption test

In a typical Rhodamine B adsorption experiment, 10 mg Fe/MC powder was added into 100 mL of 20 mgL^{-1} Rhodamine B solution. After stirring for a predetermined interval, 3 mL supernatant was analyzed. For comparison, Fe_3O_4 coated with amorphous C was also tested as adsorbent. The concentrations of Rhodamine B were quantified by UV-vis spectroscopy at 554 nm after magnetic separation. For the adsorption studies of phenol, 20 mg Fe/MC powder was added into 100 mL of 50 mgL^{-1} phenol solution under stirring for time-dependent measurements. After an interval, 3 mL supernatant was analyzed. For comparison, commercial active carbon was also tested as adsorbent. The concentrations of phenol were determined by UV-vis spectroscopy at 270 nm wavelength.

2.4 Measurements

Powder X-ray diffraction (XRD) analysis was performed on Bruke D8 Advance X-ray powder diffractometer with Cu Kα radiation (40 kV, 40 mA). Nitrogen adsorption-desorption isotherm was measured at −196 °C on ASAP 2020 volumetric analyzer. Before analysis, the sample was outgassed at 200 °C for 12 h under vacuum. The surface area was calculated using Brunauer-Emmett-Teller (BET)

method, the pore size distribution was derived from the desorption branch of the isotherm based on the Barrett-Joyner-Halenda (BJH) model and total pore volume was determined from the amount of the nitrogen adsorbed at P/P_0 ca. 0.99. Scanning electron microscopy (SEM) was recorded using a Hitachi S-4200 scanning electron microscope. Sample was mounted using a conductive carbon double-sided sticky tape, a ca. 10 nm thin coating of gold sputter was deposited onto the sample to reduce the effects of charging. Transmission electron microscopy (TEM) was recorded on a JEOL JSM-2010F electron microscope operating at 200 kV. Raman spectra were obtained on a LabRAM XploRA Raman microscope with power 0.15 mW and an argon-ion laser at an excitation wavelength of 532 nm. The Raman spectra were collected by manually placing the probe tip near the desired point of the sample on a glass slide at room temperature. The magnetization curve was measured on a Quantum Design MPMS-7 SQUID magnetometer at 300 K under a varying magnetic field. Adsorption amounts and equilibrium concentrations were quantified by Perkin Elmer Lambda 750 UV-vis spectroscopy.

3 Results and discussion

3.1 Characterizations of the sample

Figure 1 shows the powder X-ray diffraction patterns of Fe/MC and Fe/C. The small-angle XRD pattern of Fe/MC showed an intense peak at 0.9°, which was attributed to the (100) diffraction peak of the two-dimensional hexagonal mesoporous carbon, but the (110) and (200) peaks disappeared because of the incorporation of magnetic species into the porosity of mesoporous carbon (Fig. 1A). The wide-angle XRD pattern of Fe/MC showed a broad diffraction peak at 22.5° attributed to peak of amorphous carbon (Fig. 1B). The characteristic diffraction peaks at 29.98°, 35.50°, 43.15°, 53.32°, 56.83°, 62.86° and 74.32° corresponding to (220), (311), (400), (422), (511), (440) and (622) reflections, were well indexed to the face-centered cubic structured magnetite Fe_3O_4 (JCPDS file No. 19-0629). No peaks were observed in the small-angle XRD pattern of Fe/C, indicating the absence of ordered mesopore structure in Fe/C. A broad peak centered at 20.83° was observed in the wide-angle XRD pattern, indicating the amorphous carbon. The diffraction peaks characteristic of Fe_3O_4 were also clearly observed on Fe/C.

N$_2$ adsorption-desorption isotherm was measured on Fe/MC to evaluate its textural properties (Fig. 2A). A hysteresis loop at a relative pressure around 0.4–0.99 ascribed to type IV isotherm showed the presence of mesopores with pore distribution centered at 4.4 nm and 20 nm (Fig. 2A inset). The BET surface area was 742 m^2g^{-1} and the pore volume of 1.2 cm^3/g. However, there was no hysteresis loop at relative pressures of 0.4–0.99 in the sample Fe/C and its BET surface area was low at 4.2 m^2g^{-1}, further confirming the absence of mesopore in the Fe/C (Fig. 2B).

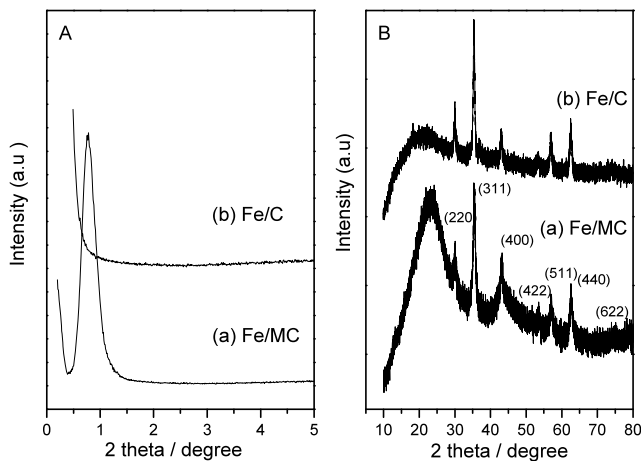**Fig. 1** (**A**) Small-angle and (**B**) wide-angle XRD patterns of Fe/MC and Fe/C

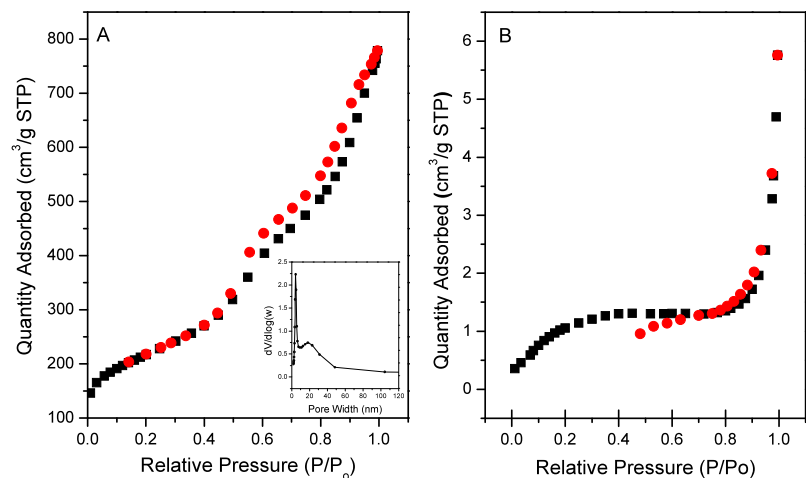**Fig. 2** Nitrogen adsorption-desorption isotherm of (**A**) Fe/MC inset: pore size distribution (**B**) Fe/C

Fig. 3 (**A**) SEM and (**B**) TEM images of Fe/MC

Fig. 4 Raman spectra of Fe/MC and mesoporous C

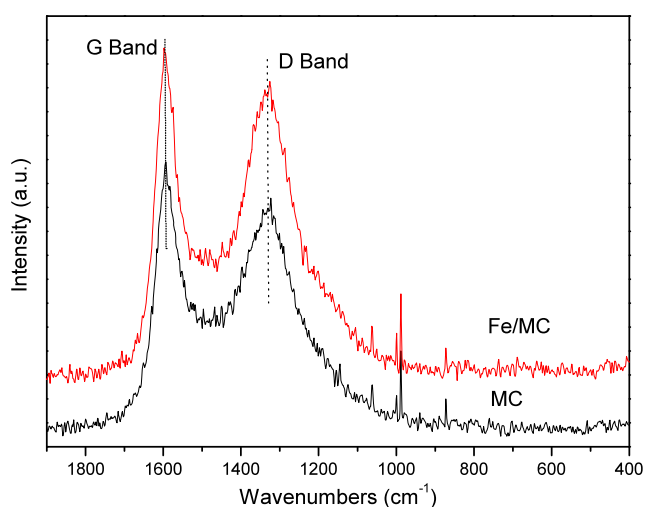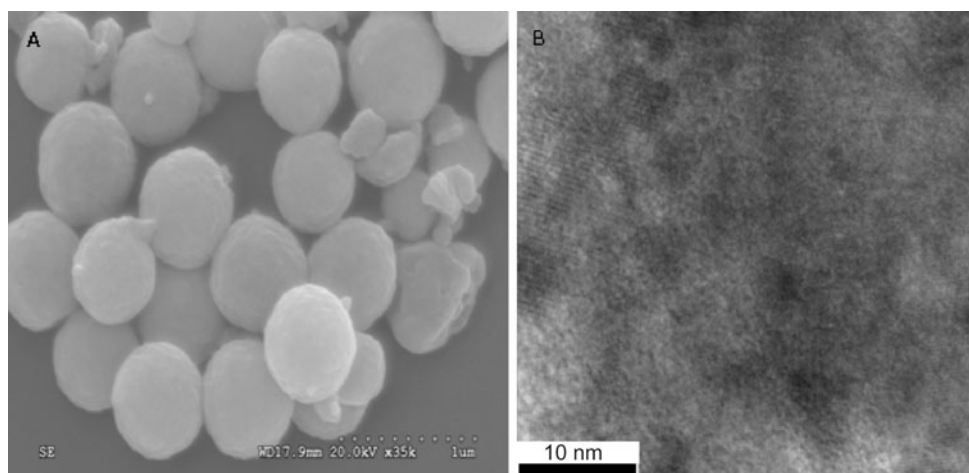**Fig. 5** M–H curve of Fe/MC

The size and morphology of as-synthesized Fe/MC were further investigated by SEM (Fig. 3A). It can be observed that Fe/MC consist of uniform spheres with sizes of $500 \sim 600$ nm. The surface of Fe/MC spheres is smooth and no magnetic nanoparticles were observed on the surface, suggesting the magnetic nanoparticles existed inside the pores of Fe/MC as shown in TEM (Fig. 3B).

To gain more information of the carbon structure, Raman spectra of mesoporous carbon and Fe/MC were measured and compared. As shown in Fig. 4, both samples exhibited the peaks at 1325 cm^{-1} and 1598 cm^{-1}. The peak at 1325 cm^{-1}, labeled as the D-band, is usually associated with the vibrations of carbon atoms with dangling bonds for the in-plane terminations of disordered graphite (Ferrari and Robertson 2001). The peak at 1598 cm^{-1} (Band G) is due to the sp^2-bonded carbon-carbon stretching (E_{2g}) mode in a two-dimensional hexagonal lattice for graphene sheet (Hu et al. 2003). The intensity ratio of the D and G bands (I_D/I_G) has a physical meaning for the crystallinity or amorphicity
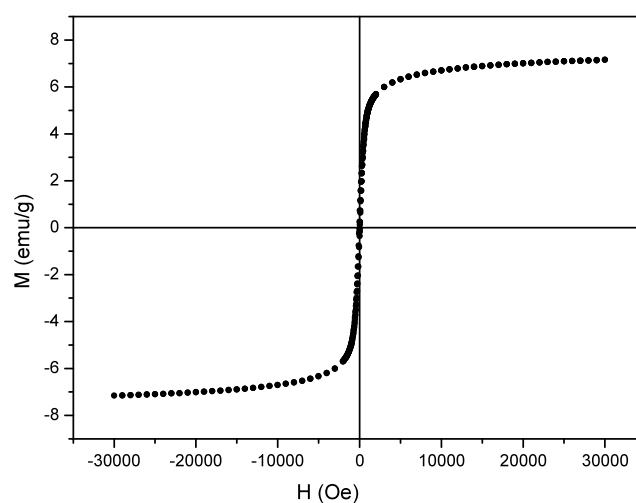
of carbon materials. The I_D/I_G of Fe/MC was slightly larger than that of the mesoporous C sample, which suggested the carbon in Fe/MC sample was more disordered because of the induced magnetic composition, in agreement with XRD result.

Superparamagnetism is the responsiveness to an applied magnetic field after removal of the applied magnetic field. The typical ferromagnetic curve of the sample Fe/MC exhibited a saturation magnetization value at 7.15 emu/g (Fig. 5). The superparamagnetic nanocomposite can be easily separated by the external magnetic field.

3.2 Adsorption of organic pollutants

Figure 6 showed the changes in Rhodamine B concentration with time after adsorption on Fe/MC and Fe/C. When 10 mg sample was added into 100 mL 20 mgL^{-1} Rhodamine B solution, over 85.45 % Rhodamine B was removed within 5 min, and Rhodamine B (99.25 %) was totally adsorbed

Fig. 6 Successive UV-vis spectra of Rhodamine B adsorption on Fe/MC and Fe/C after different time intervals
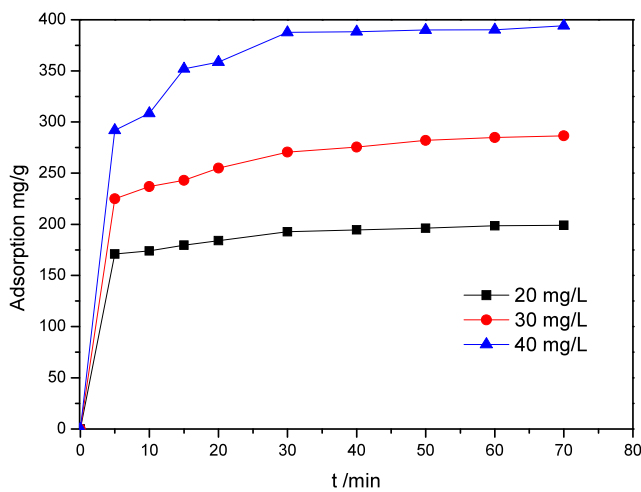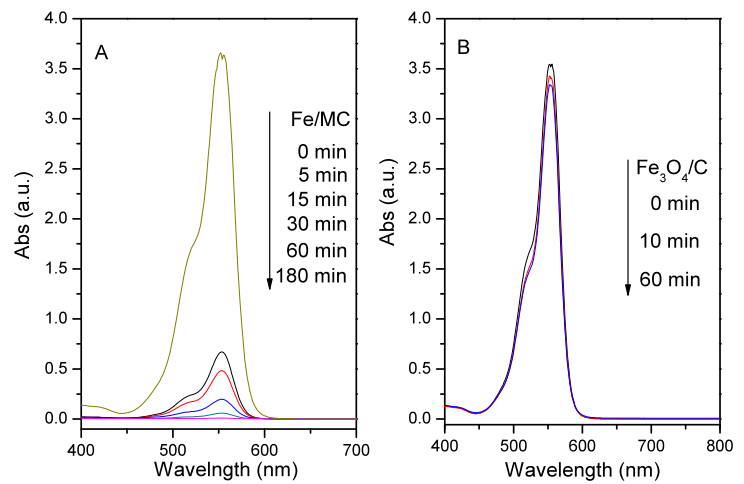

Fig. 7 The adsorption capacity of Fe/MC during Rhodamine B adsorption tests with various concentrations
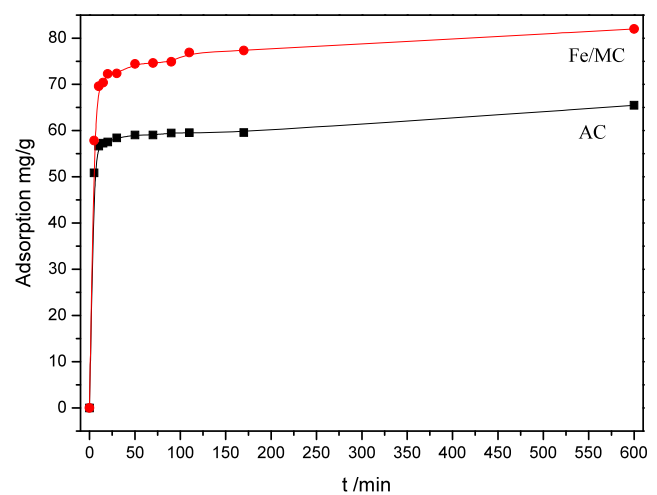
Fig. 8 The adsorption capacity of Fe/MC and AC during phenol adsorption tests

within 60 min. For comparison, Fe_3O_4 coated with amorphous carbon (BET surface area 4.2 m^2g^{-1}) showed very low adsorption capacity (7 %) within 60 min. Higher adsorption rate on Fe/MC is mainly attributed to its higher surface area, large pore volume and larger mesopores.

The adsorption of Rhodamine B solution of different concentrations v.s. time was shown in Fig. 7. The adsorption for Rhodamine B was initially very fast (before 5 min) and tapered off between 5–30 min until an adsorption equilibrium was attained (after 30 min). Dye adsorption experiments indicate that the as-prepared sample exhibits higher adsorption rate and higher capacity for dyes. Phenol, the highly toxic products of the coal carbonization, was also chosen as a model pollutant. Moreover, the adsorption amount is much higher on Fe/MC than on AC (Fig. 8). The magnetic nanocomposite can be successfully used as adsorbent for fast, convenient, and efficient removal of organic pollutants from wastewater, which will play important roles in the purification of industrial effluents.

4 Conclusions

Carbon materials are widely used as sorbents in the field of water and wastewater treatments. However, their small pore sizes and difficulty in separation from liquid phase after adsorption restrict their applications. To solve these problems, magnetic mesoporous carbon material was synthesized via a simple solvothermal route. The as-synthesized microspheres have high surface area (742 m^2/g) and large mesopore (∼4.4 nm), which show high adsorption rate and capacity for organic pollutants. Furthermore, the nanocomposite with a saturation magnetization of 7.15 emu/g is magnetically separable. The as-synthesized mesoporous carbon is an efficient magnetically separable sorbent for wastewater treatments.

References

Deng, Y.H., Cai, Y., Sun, Z.K., Zhao, D.Y.: Magnetically responsive ordered mesoporous materials: a burgeoning family of functional composite nanomaterials. Chem. Phys. Lett. **510**, 1–13 (2011)

Ferrari, A.C., Robertson, J.: Resonant: Raman spectroscopy of disordered, amorphous, and diamondlike carbon. Phys. Rev. B **64**, 75414–75427 (2001)

Gao, L.Z., Zhuang, J., Nie, L., Zhang, J.B., Zhang, Y., Gu, N., Wang, T.H., Feng, J., Yang, D.L., Perrett, S., Yan, X.: Intrinsic peroxidase-like activity of ferromagnetic nanoparticles. Nat. Nanotechnol. **2**, 577–583 (2007)

Guo, L.M., Zeng, S.Z., Li, J.T., Cui, F.M., Cui, X.Z., Bu, W.B., Shi, J.L.: An easy co-casting method to synthesize mesostructured carbon composites with high magnetic separability and acid resistance. New J. Chem. **33**, 1926–1931 (2009)

Hu, G., Cheng, M.J., Ma, D., Bao, X.H.: Synthesis of carbon nanotube bundles with mesoporous structure by a self-assembly solvothermal route. Chem. Mater. **15**, 1470–1473 (2003)

Joo, S.H., Choi, S., Oh, I., Kwak, J., Liu, Z., Terasaki, O., Ryoo, R.: Ordered nanoporous arrays of carbon supporting high dispersions of platinum nanoparticles. Nature **412**, 169–172 (2001)

Jun, S.S., Joo, S.H., Ryoo, R., Kruk, M., Jaroniec, M., Liu, Z., Ohsuna, T., Terasaki, O.: Synthesis of new, nanoporous carbon with hexagonally ordered mesostructure. J. Am. Chem. Soc. **122**, 10712–10713 (2000)

Lewis, D.L., Garrison, A.W., Wommack, K.E., Whittemore, A., Steudler, P., Melillo, J.: Influence of environmental changes on degradation of chiral pollutants in soils. Nature **401**, 898–901 (1999)

Li, X.G., Liu, R., Huang, M.R.: Facile synthesis and highly reactive silver ion adsorption of novel microparticles of sulfodiphenylamine and diaminonaphthalene copolymers. Chem. Mater. **17**, 5411–5419 (2005)

Liang, C.D., Li, Z.J., Dai, S.: Mesoporous carbon materials: synthesis and modification. Angew. Chem. Int. Ed. **47**, 3696–3717 (2008)

Liu, S.H., Lu, R.F., Huang, S.J., Lo, A.Y., Chen, S.H., Liu, S.B.: Controlled synthesis of highly dispersed platinum nanoparticles in ordered mesoporous carbon. Chem. Commun. **32**, 3435–3437 (2006)

Liu, J., Qiao, S.Z., Hu, Q.H., Lu, G.Q.M.: Magnetic nanocomposites with mesoporous structures: synthesis and applications. Small **7**, 425–443 (2011)

Lu, A.H., Schmidt, W., Matoussevitch, N., Bonnemann, H., Spliethoff, B., Tesche, B., Bill, E., Kiefer, W., Schuth, F.: Nanoengineering of a magnetically separable hydrogenation catalyst. Angew. Chem. Int. Ed. **43**, 4303–4306 (2004)

Mansouri, J., Harrisson, S., Chen, V.: Strategies for controlling biofouling in membrane filtration systems: challenges and opportunities. J. Mater. Chem. **20**, 4567–4586 (2010)

Son, S.J., Reichel, J., He, B., Schuchman, M., Lee, S.B.: Magnetic nanotubes for magnetic-field-assisted bioseparation, biointeraction, and drug delivery. J. Am. Chem. Soc. **127**, 7316–7317 (2005)

Souza, K.C., Salazar-Alvarez, G., Ardisson, J.D., Macedo, W.A., Sousa, E.M.B.: Mesoporous silica-magnetite nanocomposite. Nanotechnology **19**, 185603–185609 (2008)

Sun, Z.H., Wang, L.F., Liu, P.P., Wang, S.C., Sun, B., Jiang, D.Z., Xiao, F.-S.: Magnetically motive porous sphere composite and its excellent properties for the removal of pollutants in water by adsorption and desorption cycles. Adv. Mater. **18**, 1968–1971 (2006)

Tian, Y., Li, G.D., Gao, Q., Xiu, Y., Li, X.H., Chen, J.S.: A facile route to mesoporous carbon catalyst support modified with magnetic nanoparticles. Chem. Lett. **36**, 422–423 (2007)

Wang, X.Q., Dai, S.: A simple method to ordered mesoporous carbons containing nickel nanoparticles. Adsorption **15**, 138–144 (2009)

Wu, Z.X., Li, W., Webley, P.A., Zhao, D.Y.: General and controllable synthesis of novel mesoporous magnetic iron oxide@carbon encapsulates for efficient arsenic removal. Adv. Mater. **24**, 485–491 (2012)

Yao, J.Y., Li, L.X., Song, H.H., Liu, C.Y., Chen, X.H.: Synthesis of magnetically separable ordered mesoporous carbons from F127/Ni(H$_2$O)$_6$(NO$_3$)$_2$/resorcinol-formaldehyde composites. Carbon **47**, 436–444 (2009)

Zhai, Y.P., Dou, Y.Q., Liu, X.X., Tu, B., Zhao, D.Y.: One-pot synthesis of magnetically separable ordered mesoporous carbon. J. Mater. Chem. **19**, 3292–3300 (2009)

Zhang, Y.X., Pan, S.S., Teng, X.M., Luo, Y.Y., Li, G.H.: Bifunctional magnetic-luminescent nanocomposites: Y$_2$O$_3$/Tb nanorods on the surface of iron oxide/silica core-shell nanostructures. J. Phys. Chem. C **112**, 9623–9626 (2008)

Zhang, T., Ding, L.L., Ren, H.Q., Xiong, X.: Ammonium nitrogen removal from coking wastewater by chemical precipitation recycle technology. Water Res. **43**, 5209–5215 (2009)

Zhang, Y.X., Xu, S.C., Luo, Y.Y., Pan, S.S., Ding, H.L., Li, G.H.: Synthesis of mesoporous carbon capsules encapsulated with magnetite nanoparticles and their application in wastewater treatment. J. Mater. Chem. **21**, 3664–3671 (2011)

Zhao, D.Y., Fen, J.L., Huo, Q.S., Melosh, N., Fredrickson, G.H., Chmelka, B.F., Stucky, G.D.: Triblock copolymer syntheses of mesoporous silica with periodic 50 to 300 angstrom pores. Science **279**, 548–552 (1998)

Zhao, M., Josephson, L., Tang, Y., Weissleder, R.: Magnetic sensors for protease assays. Angew. Chem. Int. Ed. **42**, 1375–1378 (2003)